Luminescent μ-Ethynediyl and μ-Butadiynediyl Binuclear Gold(I) Complexes: Observation of $^3(\pi\pi^*)$ Emissions from Bridging C_n^{2-} Units

Chi-Ming Che,* Hsiu-Yi Chao, Vincent M. Miskowski, Yanqin Li, and Kung-Kai Cheung

Contribution from the Department of Chemistry, The University of Hong Kong, Pokfulam Road, Hong Kong SAR, China

Received May 17, 2000

Abstract: The synthesis and X-ray structural and spectroscopic characterization for $LAuC{\equiv}CAuL{\cdot}4CHCl_3$ and $LAuC{\equiv}C{-}C{\equiv}CAuL{\cdot}2CH_2Cl_2$ (**1**·4$CHCl_3$ and **2**·2CH_2Cl_2, respectively; L = PCy_3, tricyclohexylphosphine) are reported. The bridging C_n^{2-} units are structurally characterized as acetylene or diacetylene units, with C≡C distances of 1.19(1) and 1.199(8) Å for **1**·4$CHCl_3$ and **2**·2CH_2Cl_2, respectively. An important consequence of bonding to Au(I) for the C_n^{2-} moieties is that the lowest-energy electronic excited states, which are essentially acetylenic $^3(\pi\pi^*)$ in nature, acquire sufficient allowedness via Au spin−orbit coupling to appear prominently in both electronic absorption and emission spectra. The origin lines for both complexes are well-defined and are observed at 331 and 413 nm for **1** and **2**, respectively. Sharp vibronic progressions corresponding to ν(C≡C) are observed in both emission and absorption spectra. The acetylenic $^3(\pi\pi^*)$ excited state of **2** has a long lifetime (τ_0 = 10.8 μs) in dichloromethane at room temperature and is a powerful reductant ($E°[Au_2^+/Au_2^*] \leq -1.85$ V vs SSCE).

Introduction

There is growing interest in the chemical and physical properties of C_n-bridged multinuclear organometallic complexes.[1] Because of the anticipated electronic coupling between metal ions through the C_n linker both in the ground and excited states, this class of compounds has potential applications in molecular-scale electronics and nonlinear optical materials.[1] However, most studies in this area focus on synthetic and structural aspects while spectroscopic investigations, especially on the electronic transitions associated with the C_n^{2-} chain, are sparse. The electronic structure of $(CO)_5ReC{\equiv}CRe(CO)_5$ was reported by Beck and Trogler in 1990, and the lowest-energy allowed absorption at 319 nm was assigned to a $\pi(C_2^{2-}) \rightarrow \pi^*$(CO) transition.[2] A low-energy metal-to-metal charge-transfer transition across a C_n bridge, which appears in the visible region, has been independently observed by Gladysz[3] and Bruce.[4] Nevertheless, little is known about the spectroscopy and reactivity of the triplet excited states of the C_n^{2-} chains.[5]

Our objective in this work is to design and synthesize new model compounds for understanding the fundamentals of intraligand, metal-to-ligand and ligand-to-metal charge-transfer excited states associated with $M{-}C_n{-}M'$ moieties. In this regard, we envisioned that replacement of H^+ by $(R_3P)Au^+$ would afford long-lived emissive triplet excited states for the C_n^{2-} units, from which their excited-state chemistry may be developed. Because of the heavy atom effect, it is known that coordination of gold(I) to unsaturated organic species can enhance the lifetime and emission quantum yield of intraligand triplet excited states.[6]

The first μ-ethynediyl digold(I) complexes were synthesized by Cross and co-workers,[7] and their photophysical properties have been described in some instances.[6b,8] However, these luminescent complexes are supported by arylphosphine ancillary ligands. Because the lowest triplet excited state of benzene lies at 29470 cm^{-1},[9] there is a significant chance that a benzenoid state may be the lowest-energy excited state for these complexes. To eliminate spectroscopic interference from $\pi\pi^*$ states of arylphosphines, and to maintain sterically congested environments around the gold centers to restrict oligomerization via Au(I)···Au(I) interactions, we have prepared C_2- and C_4-bridged derivatives bearing tricyclohexylphosphine (PCy_3) auxiliaries, namely $(Cy_3P)AuC{\equiv}CAu(PCy_3)$ (**1**) and $(Cy_3P)AuC{\equiv}C{-}C{\equiv}CAu(PCy_3)$ (**2**). The bulky PCy_3 ligand has no interfering excited states, and these compounds exhibit luminescence spectra that can unequivocally be assigned to $^3(\pi\pi^*)$ states of the bridging C_n^{2-} units. To our knowledge, this work provides a useful entry to generate long-lived and emissive $^3(\pi\pi^*)$ states of C_n^{2-} chains

* Corresponding author. Fax: +852 2857 1586. E-mail: cmche@hku.hk.

(1) (a) Beck, W.; Niemer, B.; Wieser, M. *Angew. Chem., Int. Ed. Engl.* **1993**, *32*, 923−949. (b) Lang, H. *Angew. Chem., Int. Ed. Engl.* **1994**, *33*, 547−550. (c) Bunz, U. H. F. *Angew. Chem., Int. Ed. Engl.* **1996**, *32*, 969−971. (d) Bruce, M. I. *Coord. Chem. Rev.* **1997**, *166*, 91−119. (e) Paul. F.; Lapinte, C. *Coord. Chem. Rev.* **1998**, *178*−*180*, 431−509.

(2) Heidrich, J.; Steimann, M.; Appel, M.; Beck, W.; Phillips, J. R.; Trogler, W. C. *Organometallics* **1990**, *9*, 1296−1300.

(3) (a) Weng, W.; Bartik, T.; Gladysz, J. A. *Angew. Chem., Int. Ed. Engl.* **1994**, *33*, 2199−2202. (b) Brady, M.; Weng, W.; Zhou, Y.; Seyler, J. W.; Amoroso, A. J.; Arif, A. M.; Böhme, M.; Frenking, G.; Gladysz, J. A. *J. Am. Chem. Soc.* **1997**, *119*, 775−788.

(4) Bruce, M. I.; Low, P. J.; Costuas, K.; Halet, J. F.; Best, S. P.; Heath, G. A. *J. Am. Chem. Soc.* **2000**, *122*, 1949−1962.

(5) Dembinski, R.; Bartik, T.; Bartik, B.; Jaeger, M.; Gladysz, J. A. *J. Am. Chem. Soc.* **2000**, *122*, 810−822.

(6) (a) Li, D.; Hong, X.; Che, C. M.; Lo, W. C.; Peng, S. M. *J. Chem. Soc., Dalton Trans.* **1993**, 2929−2932. (b) Hong, X.; Cheung, K. K.; Guo, C. X.; Che, C. M. *J. Chem. Soc., Dalton Trans.* **1994**, 1867−1871.

(7) Cross, R. J.; Davison, M. F. *J. Chem. Soc., Dalton Trans.* **1986**, 411−414.

(8) Muller, T. E.; Choi, S. W. K.; Mingos, D. M. P.; Murphy, D.; Williams, D. J.; Yam, V. W. W. *J. Organomet. Chem.* **1994**, *484*, 209−224.

(9) Herzberg, G. *Molecular Spectra and Molecular Structure*: Electronic Spectra of PolyAtomic Molecules, Vol. III; Krieger: Malabar, FL, 1991.

10.1021/ja001706w CCC: $20.00 © 2001 American Chemical Society
Published on Web 05/03/2001

in fluid solutions at ambient temperature. The $^3(\pi\pi^*)$ excited state of **2** has been shown to be a powerful reductant in solution at room temperature.

Experimental Section

Materials and Reagents. $KAuCl_4$ and tricyclohexylphosphine were obtained from Strem Chemicals. 2,2′-Thiodiethanol and lithium perchlorate were purchased from Aldrich Chemicals. (Caution! *Perchlorate salts are potentially explosive and should be handled with care and in small amounts.*) 1,4-Bis(trimethylsilyl)-1,3-butadiyne was obtained from Lancaster Synthesis Ltd. The pyridinium quenchers were prepared according to literature procedures.[10] $Au(PCy_3)Cl$ was prepared from chloro(thiodiglycol)gold(I) following a standard procedure for synthesis of other phosphine derivatives.[11] Details of solvent treatment for photophysical studies have been provided earlier.[12] The other solvents used were of analytical grade.

Synthesis. $(Cy_3P)AuC{\equiv}CAuPCy_3$ (1). This complex was prepared by modification of a literature method for related derivatives.[7] Bubbling C_2H_2 through a suspension of $Au(PCy_3)Cl$ (0.76 g, 1.49 mmol) and NaOH (0.60 g, 1.49 mmol) in EtOH (100 mL) for 10 min produced a clear colorless solution. This was evaporated to dryness, and the solid residue was extracted with CH_2Cl_2 (50 mL). The volume of the filtrate was reduced to 10 mL, and diethyl ether was added to afford a white precipitate, which was collected and recrystallized by slow evaporation of a chloroform solution to produce pale yellow crystals. Yield: 32% (0.23 g). NMR ($CDCl_3$): ^{1}H δ 2.08−1.18 (m, Cy); $^{13}C\{^1H\}$ δ 147.7 (dd, $^2J_{CP}$ = 122.6 Hz, $^3J_{CP}$ = 19.0 Hz, C≡C), 33.3 (d, $^1J_{CP}$ = 27.5 Hz, Cy), 30.6 (s, Cy), 27.2 (d, $^2J_{CP}$ = 12.3 Hz, Cy), 26.0 (s, Cy); $^{31}P\{^1H\}$ δ 58.3. Raman (cm^{-1}): 2008 (s, C≡C). FAB-MS: *m/z* 980 [M^+ + H]. Anal. Calcd for $C_{38}H_{66}Au_2P_2{\cdot}3.5CHCl_3$: C, 35.80; H, 5.04%. Found: C, 35.82; H, 5.17%.

$(Cy_3P)AuC{\equiv}C{-}C{\equiv}CAu(PCy_3)$ (2). A methanolic solution (15 mL) of 1,4-bis(trimethylsilyl)-1,3-butadiyne (0.02 g, 0.10 mmol) and an excess of NaOH (0.08 g, 2.0 mmol) was stirred for 30 min. $Au(PCy_3)Cl$ (0.10 g, 0.19 mmol) was then added, and the mixture was stirred for 3 h. The white solid was collected by filtration. Pale yellow crystals were obtained by slow evaporation of diethyl ether into a dichloromethane solution. Yield: 80% (0.08 g). NMR ($CDCl_3$): ^{1}H δ 2.08−1.18 (m, Cy); $^{13}C\{^1H\}$ δ 123.8 (d, $^2J_{CP}$ = 134.1 Hz, Au−**C**≡C), 88.0 (d, $^3J_{CP}$ = 25.8 Hz, Au−C≡**C**), 33.2 (d, $^1J_{CP}$ = 27.8 Hz, Cy), 30.6 (s, Cy), 27.1 (d, $^2J_{CP}$ = 11.7 Hz, Cy), 25.9 (s, Cy); $^{31}P\{^1H\}$ δ 56.74. IR (cm^{-1}): 2145 (vw, C≡C), 2010 (vw, C≡C). Raman (cm^{-1}): 2150 (s, C≡C), 2087 (m, C≡C). FAB-MS: *m/z* 1004 [M^+ + H]. Anal. Calcd for $C_{40}H_{66}Au_2P_2{\cdot}0.2CH_2Cl_2$: C, 47.33; H, 6.56%. Found: C, 47.48; H, 6.70%.

$[Au(PCy_3)_2]ClO_4$ (3). The synthesis was similar to that of $[Au(PCy_3)_2]Cl$.[13] Tricyclohexylphospine (0.05 g, 0.18 mmol) was added to a suspension of $Au(PCy_3)Cl$ (0.10 g, 0.19 mmol) in MeOH (20 mL). After stirring for 3 h, a clear colorless solution was produced. Excess $LiClO_4$ was added, and slow evaporation to 5 mL produced colorless crystals. Yield: 88% (0.14 g). NMR (CD_3CN): ^{1}H δ 2.08−1.18 (m, Cy); $^{31}P\{^1H\}$ δ 65.41. IR (cm^{-1}): 2928, 2852 (s, Cy), 1089 (s, br, ClO_4^-). FAB-MS: *m/z* 757 [$Au(PCy_3)_2^+$]. Anal. Calcd for $C_{36}H_{66}AuClO_4P_2$: C, 50.44; H, 7.77%. Found: C, 50.18; H, 7.94%.

Instrumentation. Details of physical instrumentation are available in the Supporting Information. The solution emission quantum yields were measured by the method of Demas and Crosby[14] using quinine sulfate in degassed 0.1 N sulfuric acid as standard (ϕ_r = 0.546). Emission quantum yields of powder samples were measured using the method of Wrighton and co-workers[15] with KBr as the standard and calculated by $\phi = E/(R_{std} - R_{smpl})$, where E is the area under the corrected emission curve of the sample and R_{std} and R_{smpl} are the corrected areas under the diffuse reflectance curves of the nonabsorbing standard and the sample, respectively, at the excitation wavelength. Emission quenching was performed by lifetime measurements, and the quenching rate constant, k_q, was deduced from the plot of $1/\tau$ versus [Q] according to the Stern−Volmer equation $\tau_0/\tau = 1 + k_q\tau_0[Q]$, where τ_0 and τ are the respective emission lifetimes in the absence and presence of quencher Q.

Table 1. Crystallographic Data for **1**·$4CHCl_3$ and **2**·$2CH_2Cl_2$

	1·$4CHCl_3$	**2**·$2CH_2Cl_2$
formula	$Au_2C_{38}H_{66}P_2{\cdot}4CHCl_3$	$Au_2C_{40}H_{66}P_2{\cdot}2CH_2Cl_2$
M (g/mol)	1456.33	1172.71
crystal system	monoclinic	triclinic
space group	$P2_1/n$ (no. 14)	$P\bar{1}$ (no. 2)
color of crystal	pale yellow	pale yellow
a (Å)	10.500(2)	9.268(1)
b (Å)	18.464(3)	9.985(2)
c (Å)	15.011(2)	13.971(3)
α (deg)	90	104.81(2)
β (deg)	100.12(2)	90.24(2)
γ (deg)	90	109.30(2)
V (Å^3)	2864.9(8)	1174(1)
Z	2	1
F(000)	1428	578
μ (cm^{-1})	57.75	65.85
D_c (gcm^{-3})	1.688	1.658
$2\theta_{max}$ (°)	51.1	50.1
no. of unique refins	5102	4114
no. of reflns with $I > 3\sigma(I)$	4004	3717
no. of parameters	262	226
R^a, $R_w{}^b$	0.043, 0.061	0.029, 0.039
goodness-of-fit	1.91	1.95
residual ρ, e Å^{-3}	+1.25, −1.11	+0.95, −1.10

^{a} $R = \Sigma||F_o| - |F_c||/\Sigma|F_o|$. ^{b} $R_w = [\Sigma w(|F_o| - |F_c|)^2/\Sigma w|F_o|^2]^{1/2}$.

X-ray Crystallography. Crystals of **1**·$4CHCl_3$ and **2**·$2CH_2Cl_2$ were grown by slow evaporation of a chloroform solution and by diffusion of diethyl ether into a dichloromethane solution, respectively. Crystal data and details of collection and refinement are listed in Table 1. For **1**·$4CHCl_3$, diffraction experiments were performed at 301 K on a MAR diffractometer with a 300 mm image plate detector using graphite monochromatized Mo Kα radiation (λ = 0.71073 Å). For **2**·$2CH_2Cl_2$, diffraction experiments were performed at 301 K on a Rigaku AFC7R diffractometer (λ = 0.71073 Å, $\omega-2\theta$ scans). Details of structure refinements are available in Supporting Information.

Results

Syntheses and Characterization. The syntheses of μ_2-C_n binuclear metal complexes have already been subjected to extensive studies[1,3−5,16−20] notably by Gladysz and co-workers. Many μ_2-C_2 and μ_2-C_4 binuclear derivatives incorporating the late transition metal ions have been reported.[1] Synthetic methods for the former typically employ C_2H_2 or metal ethynyl species as the C_2 source.[7,8,21] For μ_2-C_4 complexes, terminal alkyne coupling reactions between two metal ethynyl moieties[22] or the

(10) Che, C. M.; Kwong, H. L.; Poon, C. K.; Yam, V. W. W. *J. Chem. Soc., Dalton Trans.* **1990**, 3215−3219.
(11) Al-sa'ady, A. K.; Mcauliffe, C. A.; Parish, R. V.; Sandbank, J. A. *Inorg. Synth.* **1985**, *23*, 191−194.
(12) Lai, S. W.; Chan, M. C. W.; Cheung, T. C.; Peng, S. M.; Che, C. M. *Inorg. Chem.* **1999**, *38*, 4046−4055.
(13) Muir, J. A.; Muir, M. M.; Pulgar, L. B.; Jones, P. G.; Sheldrick, G. M. *Acta Crystallogr.* **1985**, *C41*, 1174−1176.
(14) Demas, J. N. G.; Crosby, A. *J. Phys. Chem.* **1971**, *75*, 991−1024.
(15) Wrighton, M. S.; Ginley, D. S.; Morse, D. L. *J. Phys. Chem.* **1974**, *78*, 2229−2233.
(16) Peters, T. B.; Bohling, J. C.; Arif, A. M.; Gladysz, J. A. *Organometallics* **1999**, *18*, 3261−3263.
(17) Sakurai, A.; Akita, M.; Moro-oka, Y. *Organometallics* **1999**, *18*, 3241−3244.
(18) Yam, V. W. W.; Lau, V. C. Y.; Cheung, K. K. *Organometallics* **1996**, *15*, 1740−1744.
(19) Gil-Rubio, J.; Laubender, M.; Werner, H. *Organometallics* **1998**, *17*, 1202−1207.
(20) Bruce, M. I.; Hall, B. C.; Kelly, B. D.; Low, P. J.; Skelton, B. W.; White, A. H. *J. Chem. Soc., Dalton Trans.* **1999**, 3719−3728.
(21) Muller, T. E.; Mingos, D. M. P.; Williams, D. J. *J. Chem. Soc., Chem. Commun.* **1994**, 1787−1788.
(22) (a) Zhou, Y.; Seyler, J. W.; Weng, W.; Arif, A. M.; Gladysz, J. A. *J. Am. Chem. Soc.* **1993**, *115*, 8509−8510. (b) Brady, M.; Weng, W.; Gladysz, J. A. *J. Chem. Soc., Chem. Commun.* **1994**, 2655−2656.

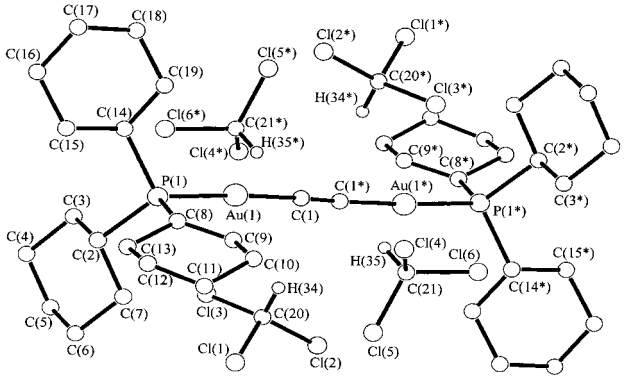

Figure 1. Perspective view of $(Cy_3P)AuC{\equiv}CAu(PCy_3)\cdot 4CHCl_3$ (**1**·$4CHCl_3$), showing the C−H···π interactions with $CHCl_3$ molecules. Selected bond distances (Å) and angles (deg): Au(1)−P(1) 2.287(2), Au(1)−C(1) 2.000(7), C(1)−C(1*) 1.19(1), P(1)−Au(1)−C(1) 176.3(2), Au(1)−C(1)−C(1*) 178.3(9), Au(1)−P(1)−C(2) 109.6(2), Au(1)−P(1)−C(8) 113.5(3), Au(1)−P(1)−C(14) 112.3(3).

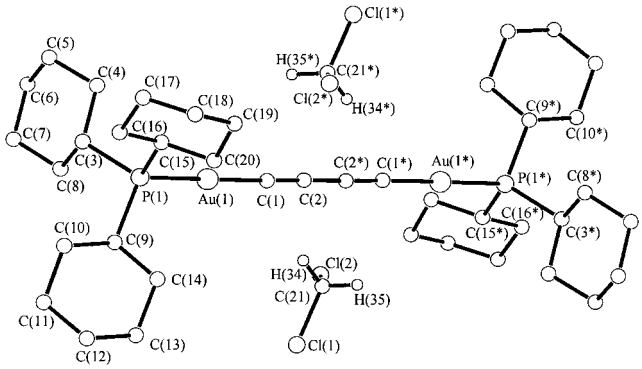

Figure 2. Perspective view of $(Cy_3P)AuC{\equiv}C{-}C{\equiv}CAu(PCy_3)\cdot 2CH_2Cl_2$ (**2**·$2CH_2Cl_2$). Selected bond distances (Å) and angles (deg): Au(1)−P(1) 2.286(1), Au(1)−C(1) 2.012(6), C(1)−C(2) 1.199(8), C(2)−C(2*) 1.37(1), C(1)−C(2)−C(2*)178.7(9), P(1)−Au(1)−C(1) 179.4(2), Au(1)−C(1)−C(2) 175.8(6), Au(1)−P(1)−C(3) 111.8(2), Au(1)−P(1)−C(9) 111.8(2), Au(1)−P(1)−C(15) 109.5(2).

reactions of metal chloride derivatives with 1,4-bis(trimethylsilyl)-1,3-butadiyne[4,20] have been used. The ethynediylgold(I) complex $(Cy_3P)AuC{\equiv}CAu(PCy_3)$ (**1**) was prepared using a modification of the procedure reported by Cross and Davison.[7] Thus, a suspension of $Au(PCy_3)Cl$ in ethanol reacts with ethyne gas in the presence of NaOH to produce $(Cy_3P)AuC{\equiv}CAu(PCy_3)$; the rapid reaction produces a clear solution from which **1** is easily isolated. The Raman spectrum of **1** shows a very strong peak at 2008 cm^{-1}, which is characteristic of a C≡C stretch. Hence, the bridging C_2 ligand of **1** can be confidently classified as an ethynediyl unit.[1a] The $^{31}P\{^1H\}$ NMR spectrum indicates a single environment for the phosphine ligands at 58.3 ppm, and this is slightly downfield from that for $Au(PCy_3)Cl$ (55.21 ppm). Evidently, the electronic effect of the ethynediyl group, as transmitted through Au(I), is not very different from that for Cl. The $^{13}C\{^1H\}$ NMR spectrum shows a doublet of doublets centered at 147.7 ppm for the ethynediyl unit, with coupling to two phosphorus nuclei ($^2J_{CP}$ = 122.6 and $^3J_{CP}$ = 19.0 Hz).

Complex **2** was synthesized by the reaction of 2 equiv of $Au(PCy_3)Cl$ with 1,4-bis(trimethylsilyl)-1,3-butadiyne in the presence of NaOH in MeOH. In the Raman spectrum of **2**, the two peaks at 2150 and 2087 cm^{-1} are attributed to ν(C≡C) modes. The $^{13}C\{^1H\}$ NMR spectrum of **2** shows two doublets centered at 88.0 and 123.8 ppm. The former is assigned to C(2) with $^3J_{CP}$ = 25.8 Hz, and the latter is assigned to C(1) with $^2J_{CP}$ = 134.1 Hz (for nomenclature, see Figure 2).

To assist in the spectra interpretation of **1** and **2**, the bis(phosphine) complex $[Au(PCy_3)_2]ClO_4$ (**3**) was prepared. The $^{31}P\{^1H\}$ NMR spectrum of **3** shows a single peak at 65.41 ppm.

Crystal Structures. Figure 1 shows the perspective view of **1**·$4CHCl_3$, which has a crystallographic rotation center located at the center of the ethynediyl unit. The gold atoms reside in a virtually linear two-coordinate environment, and are bridged by a C_2^{2-} ligand with P−Au−C and Au−C−C angles of 176.3(2) and 178.3(9)°, respectively. The C≡C bond length is 1.19(1) Å; this bond length, as well as those of the Au−C (2.000(7) Å) and Au−P (2.287(2) Å) bonds, are almost identical to those in the PPh_3 analogue, $(Ph_3P)Au{-}C{\equiv}C{-}Au(PPh_3)\cdot 2C_6H_6$ (1.19(2), 2.00(1), and 2.280(3) Å, respectively).[23] As observed for $(NpPh_2P)Au{-}C{\equiv}C{-}Au(PNpPh_2)\cdot 2CHCl_3$ (1.222(16), 1.983(8), and 2.277(2) Å, respectively)[8] and $(Np_2PhP)Au{-}C{\equiv}C{-}Au(PNp_2Ph)\cdot 6CHCl_3$ (1.225(34), 1.986(17), and 2.289(5) Å, respectively) (Np = naphthyl),[21] there are cocrystallized $CHCl_3$ molecules which are positioned with their C−H bonds directed orthogonally toward the center of the ethynediyl unit in the crystal lattice of **1**·$4CHCl_3$. The distances of H(34) and H(35) to the center of the ethynediyl bond are ca. 2.4 and 2.5 Å, respectively. The H(34)−H(34*) and H(35)−H(35*) vectors are inclined by 86 and 88° respectively to the C(1)≡C(1*) bond and constitute a pseudo-octahedral arrangement. Intermolecular distances of H(34) and H(35) to C(1) and C(1*) range between 2.5 and 2.6 Å. The T-shaped intermolecular CH···π interactions in **1**·$4CHCl_3$ are comparable in nature to those in $(NpPh_2P)Au{-}C{\equiv}C{-}Au(PNpPh_2)\cdot 2CHCl_3$ (2.42 Å)[8] and $(Np_2PhP)Au{-}C{\equiv}C{-}Au(PNp_2Ph)\cdot 6CHCl_3$ (2.50 and 2.58 Å, respectively).[21] These interactions can be rationalized in terms of the acidity of the C−H proton in $CHCl_3$ and back-donation of electron density from the gold atom to the C≡C bond. Theoretical calculations on $(H_3P)Au{-}C{\equiv}C{-}Au(PH_3)\cdots CHCl_3$ predicted interaction distances of 2.17 and 2.01 Å and interaction energy in the range of 25 kJ mol^{-1}, values which are typical for classical hydrogen-bonded systems.[24]

For each molecule of $(Cy_3P)AuC{\equiv}C{-}C{\equiv}CAu(PCy_3)$ (**2**), there are two cocrystallized CH_2Cl_2 molecules (Figure 2). Two $Au(PCy_3)$ fragments are bridged by a nearly linear C_4 unit, with Au−C(1)−C(2) and C(1)−C(2)−C(2*) angles of 175.8(6) and 178.7(9)°, respectively. The Au−P and Au−C bond lengths are 2.286(1) and 2.012(6) Å, respectively, and are comparable to those in ethynediyl digold(I) complexes.[8,21,23] The C(1)−C(2) and C(2)−C(2*) bond distances of the C_4 unit are 1.199(8) and 1.37(1) Å, respectively, which are similar to those in the related C_4-bridged bimetallic complexes (*SS*,*RR*)-$[\{Re(\eta^5\text{-}C_5Me_5)(NO)(PPh_3)\}_2(\mu\text{-}C{\equiv}C{-}C{\equiv}C)]$ (1.202(7), and 1.389(5) Å, respectively),[22a] $[\{Fe(\eta^5\text{-}C_5Me_5)(\eta^2\text{-dppe})\}_2(\mu\text{-}C{\equiv}C{-}C{\equiv}C)][PF_6]$ (1.236(9) and 1.36(1) Å, respectively),[25] $[\{Rh(P^iPr_3)_2(CO)\}_2(\mu\text{-}C{\equiv}C{-}C{\equiv}C)]$ (1.205(5) and 1.388(7) Å, respectively),[26] and $[\{Re(^tBu_2bpy)(CO)_3\}_2(\mu\text{-}C{\equiv}C{-}C{\equiv}C)]$ (1.19(2) and 1.43(4) Å, respectively).[18] There are likely to be CH···π interactions between the CH_2Cl_2 molecules and the C_4 unit, as indicated by the locations of the solvent molecules, but because of disorder of the CH_2Cl_2 molecules in the X-ray refinement process, these cannot be quantified.

(23) Bruce, M. I.; Grundy, K. R.; Liddell, M. J.; Snow, M. R.; Tiekink, R. T. *J. Organomet. Chem.* **1988**, *344*, C49−C52.

(24) Fan, M. F.; Lin, Z.; McGrady, J. E.; Mingos, D. M. P. *J. Chem. Soc., Perkin Trans. 2* **1996**, 563−568.

(25) Narvor, N. L.; Toupet, L.; Lapinte, C. *J. Am. Chem. Soc.* **1995**, *117*, 7129−7138.

(26) Gevert, O.; Wolf, J.; Werner, H. *Organometallics* **1996**, *15*, 2806−2809.

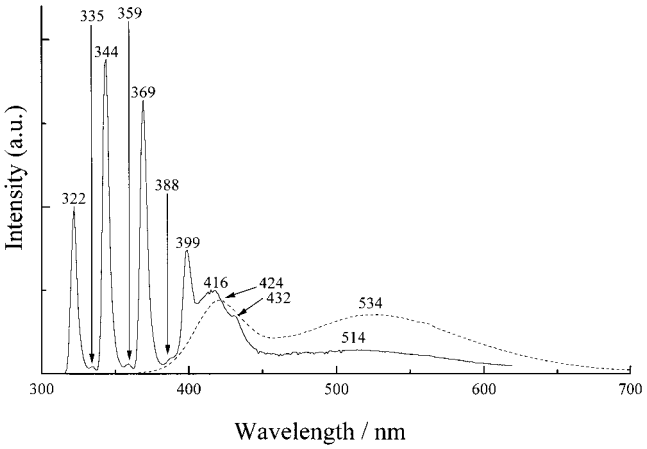

Figure 3. Normalized emission spectra of $(Cy_3P)AuC{\equiv}CAu(PCy_3)\cdot 4CHCl_3$ (**1**·$4CHCl_3$) in the solid state at 298 K (dashed line) and 77 K (solid line) with excitation wavelength at 280 nm.

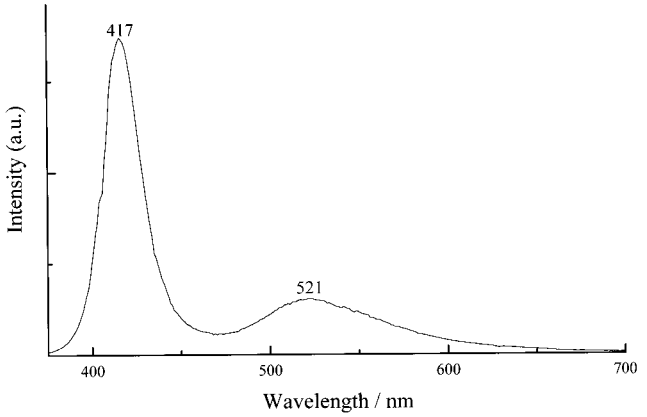

Figure 4. Emission spectrum of $(Cy_3P)AuC{\equiv}CAu(PCy_3)$ (**1**) in MeOH/EtOH (4:1 v/v) at 77 K with excitation wavelength at 280 nm.

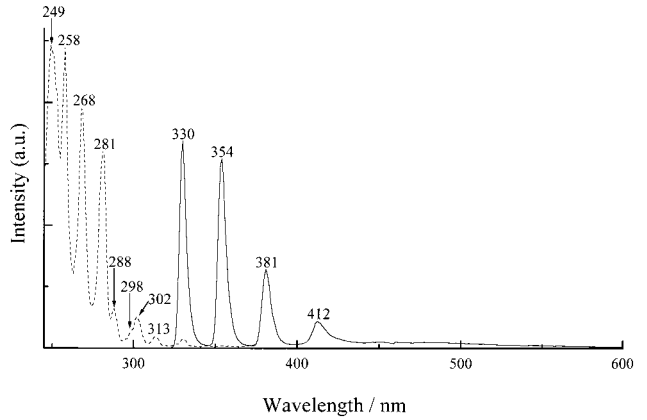

Figure 5. Emission (solid line) and excitation (dashed line) spectra of $(Cy_3P)AuC{\equiv}CAu(PCy_3)$ (**1**) in glassy *n*-butyronitrile at 77 K. The emission wavelength was monitored at 381 nm.

Electronic Emission and Absorption Spectra. Emission spectra of **1** and **2** are presented in Figures 3−6, and the data are summarized in Table 2. For solutions of **2** in moderately polar solvents (CH_2Cl_2 and THF) and for microcrystalline solids of **1**·$4CHCl_3$ at 77 K and **2**·$2CH_2Cl_2$ at room temperature, well-resolved vibronic structures are shown in the emission spectrum. Indeed, extremely sharp progressions are observed in a single frequency ∼2000 cm^{-1} which is assigned to the symmetric υ(C≡C) mode. The emission spectrum of **2** in CH_2Cl_2 (Figure 6) is very similar to that of **1** in *n*-butyronitrile glass (77 K)

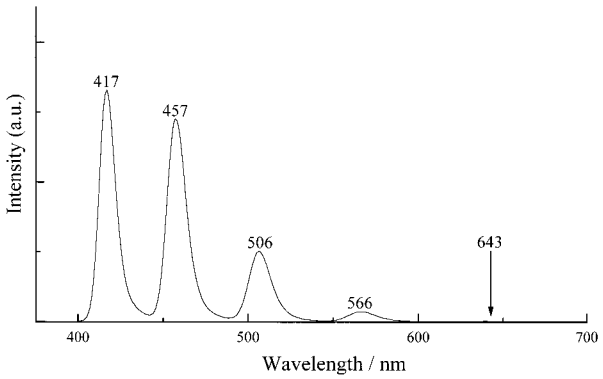

Figure 6. Emission spectrum of $(Cy_3P)AuC{\equiv}C{-}C{\equiv}CAu(PCy_3)$ (**2**) in degassed CH_2Cl_2 solution at 298 K with excitation wavelength at 364 nm.

except that it is red-shifted by ∼6000 cm^{-1} (the progression frequency ∼2100 cm^{-1}). Complex **1**·$4CHCl_3$ exhibits, in most media, two broad emissions centered at λ_{max} 415 and 530 nm which are completely dominant for the room-temperature solid and in alcoholic glass (Figures 3 and 4).

It is noteworthy that we have been able to observe the sharp-line emissions of **1** in *n*-butyronitrile glass and **2** in fluid solutions. Luminescence excitation spectra for these emissions, as illustrated in Figure 5 for **1**, are in excellent agreement with absorption spectra. Absorption spectra of **1** and **2** in CH_2Cl_2 are shown in Figures 7 and 8, and the data are collected in Table 2. The absorption spectrum of **3** (see Supporting Information) is in good agreement with those reported by Mason and co-workers for analogous Au(I) trialkylphosphine complexes.[27] Thus, even at very high concentrations (∼10^{-2} mol dm^{-3}), no bands could be detected at lower energies relative to the 251 nm band, and absorbance is negligible beyond 265 nm. In contrast, **1** and **2** exhibit well-defined absorption bands extending to much longer wavelengths (>260 nm). Indeed, the absorption bands above 260 nm are absent from the spectrum of **3**. The lowest-energy feature in the room-temperature spectrum of **1** in CH_2Cl_2 (Figure 7) is a weak ($\epsilon \approx 50$ dm^3 mol^{-1} cm^{-1}), narrow absorption band at 331 nm that corresponds extremely well to the 330 nm origin line in both the 77 K *n*-butyronitrile emission and excitation spectra (Figure 5). Evidently these features represent the origin lines of an electronic transition that is electronic-dipole allowed, albeit weakly; the negligible Stokes shift is a consequence of the narrow line-width.

The excitation spectrum of complex **1** (Figure 5) at 77 K is better resolved than the room-temperature absorption spectrum. A band at 313 nm and a shoulder at 298 nm have appropriate intensities relative to the origin line and thus correspond to one and two quanta of the excited-state progression frequency; this assignment hence implies a very substantial decrease of the vibrational frequency in the excited state, to ∼1700 cm^{-1}. Two additional low-energy bands at 302 and 288 nm are resolved in the excitation spectrum. These are more intense than the features discussed above ($\epsilon \approx 330$ dm^3 mol^{-1} cm^{-1} for the 303 nm band, Figure 7), and their positions do not fit into a vibrational progression based upon the 330 nm origin. We therefore attribute the 302 nm feature to another electronic origin. The separation between the 302 and 288 nm bands of ∼1600 cm^{-1} suggests that this state distorts along the same vibrational coordinate as the lowest-energy state and is therefore electronically related.

(27) (a) Savas, M. M.; Mason, W. R. *Inorg. Chem.* **1987**, *26*, 301−307. (b) Jaw, H. R. C.; Mason, W. R. *Inorg. Chem.* **1989**, *28*, 4370−4373. (c) Chastain, S. K.; Mason, W. R. *Inorg. Chem.* **1982**, *21*, 3717−3721.

Table 2. Photophysical Data for Complexes **1**−**3**

complex	medium (*T*/K)	λ^{abs}/nm (ϵ_{max}/dm^3 mol^{-1} cm^{-1})	λ^{em}/nm (τ/μs)[a]	ϕ_{em}[a]
1	CH_2Cl_2 (298)	239 (47260), 256 (55020), 270 (6840), 283 (3500), 303 (330), 315 (sh, 120), 331 (50)		
	solid (298)		424 (0.28), 534 (0.33)	0.058
	solid (77)		322 (2.9), 335, 344, 359, 369, 388, 399, 416, 432, 514 (6.7)	
	MeOH/EtOH (4:1 v/v) (77)		417 (1.4), 521 (5.5)	
	n-butyronitrile (77)		330 (4.6), 354, 381, 412 (1.2)	
2	CH_2Cl_2 (298)	245 (77930), 252 (sh, 27350), 264 (119880), 291 (1770), 309 (1410), 328 (580), 339 (sh, 130), 361 (80), 381 (40), 413 (20)	417 (10.8), 457, 506, 566, 643	0.21
	THF (298)	246 (49100), 256 (sh, 53800), 270 (103340), 295 (2700), 313 (2320), 334 (1150), 359 (80), 368 (90), 386 (50), 418 (40), 434 (20)	419 (2.4), 461, 511, 573, 650	0.025
	solid (298)		417 (25), 457, 507, 566, 643	0.17
3	CH_2Cl_2 (298)	239 (2200), 251 (1810)		

[a] Errors for τ and ϕ_{em} are estimated to be ±5% and 10%, respectively.

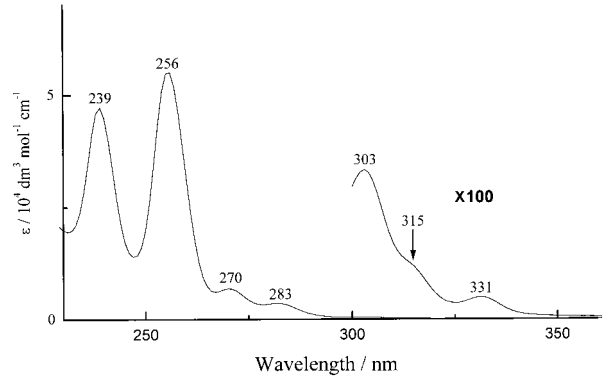

Figure 7. Absorption spectrum of $(Cy_3P)AuC{\equiv}CAu(PCy_3)$ (**1**) in CH_2Cl_2 solution at 298 K.

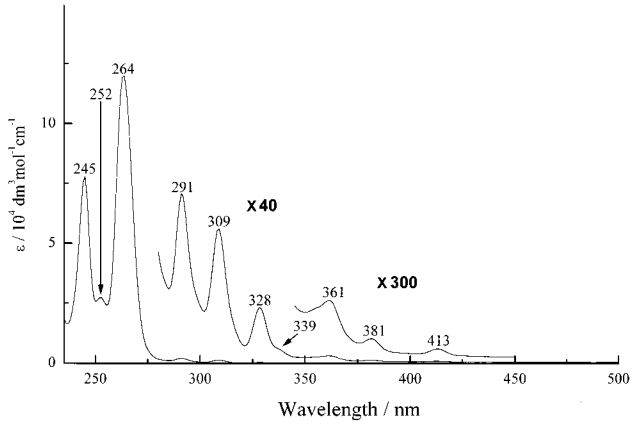

Figure 8. Absorption spectrum of $(Cy_3P)AuC{\equiv}C{-}C{\equiv}CAu(PCy_3)$ (**2**) in CH_2Cl_2 solution at 298 K.

At higher energies, four absorption bands of significantly greater intensity are observed. The two bands of **1** at 239 and 256 nm initially appear to correspond to the two bands of **3** at 239 and 251 nm, but the extinction coefficients of the bands of **1** are too high for such a correlation. We suggest instead that the two bands at 270 and 283 nm for **1** correlate to the lowest-energy bands of **3**. The very intense bands of **1** at 239 and 256 nm can then be correlated to bands in **3** and related complexes[27] that appear at $\lambda < 210$ nm.

The absorption spectrum of **2** (Figure 8) is similar to that of **1**, but with additional complexities. Bands at 245, 264, 291, and 309 nm are similar to the bands of **1** that we have assigned to red-shifted [5d(Au)] → [6p(Au), π*(phosphine)] transitions. In addition, a weak, vibronically structured absorption system is found that is very similar to that of **1** but, like the emission, red-shifted by ∼6000 cm^{-1}. As before, there is good zero-zero overlap between the absorption and emission spectra. We once again infer two electronic origins at 413 and 361 nm for **2**. The only band in the absorption spectrum of **2** that does not have an obvious blue-shifted analogue in the spectrum of **1** appears at 328 nm ($\epsilon \approx 580$ dm^3 mol^{-1} cm^{-1}). It is possible that the corresponding band for **1** is obscured by Au d → p transitions.

Reactivity and Photoredox Properties of the Butadiynediyl $^3(\pi\pi^*)$ State of Complex 2. Although **1** is nonemissive in solution at room temperature, **2** displays a long-lived acetylenic $^3(\pi\pi^*)$ emission in dichloromethane and tetrahydrofuran solutions (Table 2). Like the emissions of aromatic organic molecules, the emission lifetime of **2** is affected by complex concentration. A linear relationship ($R = 0.93$) can be obtained by plotting $1/\tau$ versus [**2**] in dichloromethane; the self-quenching rate constant ($k_q = 8.2 \times 10^7$ dm^3 mol^{-1} s^{-1}) and lifetime at infinite dilution ($\tau_0 = 10.8$ μs) are determined from the slope and reciprocal intercept of the plot (see Supporting Information). However, even in concentrated solutions of **2** (up to ∼10^{-3} mol dm^{-3}) in dichloromethane, there is no change in the emission peak maxima, and no additional low-energy band attributable to excimer emission is observed. The solvent effect on the photoluminescence of complex **2** has been examined in two solvents due to its general low solubility. Changing the solvent from dichloromethane to tetrahydrofuran decreases both the lifetime and quantum yield (Table 2).

The acetylenic $^3(\pi\pi^*)$ excited state of **2** is a powerful photoreductant. The emission of **2** in dichloromethane/acetonitrile (1:1 v/v) solution is oxidatively quenched by a series of pyridinium acceptors (A^+) of various reduction potentials.[28] The quenching rate constants are summarized in Table 3. As shown in Table 3, the rate constants decrease with the $E°[A^+/A]$ values suggesting an electron-transfer mechanism for the quenching reactions (eq 1).

$$[(Cy_3P)Au{-}C{\equiv}C{-}C{\equiv}C{-}Au(PCy_3)] + A^+ \rightarrow [(Cy_3P)Au{-}C{\equiv}C{-}C{\equiv}C{-}Au(PCy_3)]^+ + A \quad (1)$$

Notably, even with 2,6-dimethyl-4-methoxy-*N*-methylpyridin-

(28) Marshall, J. L.; Stobart, S. R.; Gray, H. B. *J. Am. Chem. Soc.* **1984**, *106*, 3027−3029.

Table 3. Bimolecular Rate Constants for the Oxidative Quenching of **2** by Pyridinium Acceptors in Degassed Dichlomethane/Acetonitrile (1:1 v/v) (0.1 mol dm^{-3} $^nBu_4NPF_6$) at 298 K

quencher[a]	$E°$ (A^+/A) (vs SSCE)[b]	k_q ($dm^3\,mol^{-1}\,s^{-1}$)	k_q' ($dm^3\,mol^{-1}\,s^{-1}$)[c]	$\ln k_q'$
N,*N*′-dimethyl-4,4′-pyridinium	−0.45	5.37×10^9	9.72×10^9	23.00
4-cyano-*N*-methylpyridinium	−0.67	4.77×10^9	7.92×10^9	22.79
4-methoxycarbonyl-*N*-methylpyridinium	−0.78	4.28×10^9	6.65×10^9	22.62
4-amido-*N*-ethylpyridinium	−0.93	2.56×10^9	3.25×10^9	21.90
3-amido-*N*-benzylpyridinium	−1.07	2.03×10^9	2.44×10^9	21.62
3-amido-*N*-methylpyridinium	−1.14	1.64×10^9	1.90×10^9	21.37
2,6-dimethyl-*N*-methylpyridinium	−1.52	2.76×10^9	3.58×10^9	22.00
2,4,6-trimethyl-*N*-methylpyridinium	−1.67	1.10×10^9	1.21×10^9	20.91
2,6-dimethyl-4-methoxy-*N*-methylpyridinium	−1.88	4.75×10^8	4.95×10^8	20.02

[a] All quenchers are hexafluorophosphate salts. [b] From ref 28. [c] $(1/k_q') = (1/k_q) - (1/k_d)$ where k_d is the diffusion-limited rate constant, taken to be 1.2×10^{10} dm^3 mol^{-1} s^{-1}. Errors for k_q and k_q' are estimated to be ±5%.

ium hexafluorophosphate which has a reduction potential of −1.87 V,[29] the quenching rate constant just remains high (4.95×10^8 mol^{-1} dm^3 s^{-1}). Because the range of the quenching rate constants is not wide, the excited-state potential of $E°[Au_2^+/Au_2*]$ (Au_2 = **2**) cannot be accurately determined by applying $\ln k_q'$ versus $E°[A^+/A]$ according to the Marcus equation.[30] However, $E°[Au_2^+/Au_2*]$ can be estimated by the equation: $E°[Au_2^+/Au_2*] = E°[Au_2^+/Au_2] - E_{0-0}$, where E_{0-0} is calculated spectroscopically (2.97 eV), and $E°[Au_2^+/Au_2]$ is obtained from cyclic voltammetry. Complex **2** is electrochemically inactive toward reduction but undergoes irreversible oxidation at 1.12 V. Thus $E°[Au_2^+/Au_2]$ is estimated to be ≤1.12 V vs SSCE (sodium chloride saturated calomel electrode),[31] and $E°[Au_2^+/Au_2*]$ is calculated at ≤−1.85 V vs SSCE. Flash photolysis experiments with excitation at 355 nm of a dichloromethane/acetonitrile (1:1 v/v) solution containing complex **2** (~10^{-3} mol dm^{-3}) and MV^{2+} (methyl viologen) (~10^{-2} mol dm^{-3}) revealed a signal corresponding to the formation of MV^+ (λ_{max} = 390 and 600 nm) 2 μs after the laser flash. However, complex **2** is unstable upon rendering photoirradiation, thus making photochemical reactivity studies difficult.

Discussion

Ethynediyl-bridged complexes $L_nM-C_2-ML_n$ with bond distances consistent with C_2 bond orders ranging from three (M−C bond order of one) to two (M−C bond order of two)[32] to one (M−C bond order of three)[33] have been reported. The vast majority, including complex **1** of the present study, correspond to the first case[1] and may be regarded as "dimetalated hydrocarbons".[1a]

There are several significant spectroscopic consequences of the bridging C_n^{2-} ligands:

(1) The [5d(Au)] → [6p(Au), π*(phosphine)] transitions, which are well-resolved for complexes **1** and **2**, are strongly red-shifted from those of the bis(phosphine) derivative **3**. According to Mason and co-workers, the 239 and 251 nm band of **3** can be assigned to [5d(Au)] → [6p(Au), π*(phosphine)] transitions that have singlet−triplet parentage, but spin−orbit mixing is large.[27] These two transitions can be correlated to the absorption bands at 270 and 283 nm for **1**, and 291 and 309 nm for **2**. This assignment is made by considering the extinction coefficients of these transitions. In contrast, the [5d(Au)] → [6p(Au), π*(phosphine)] transitions with singlet−singlet parentage, which are an order of magnitude more intense, are located at <210 nm,[27] and the highly intense bands at 239 and 256 nm for **1**, and at 245 and 264 nm for **2**, can be ascribed to this type of transition. These assignments imply that all [5d(Au)] → [6p(Au), π*(phosphine)] transitions for **1** are red-shifted by ~5000 cm^{-1} compared to those for **3**. For **2**, red-shifts of ~3000 and ~1000 cm^{-1} for the singlet−triplet and singlet−singlet parentage transitions, respectively, are apparent. In principle, such an effect may arise from two possible mechanisms. First, π- (or σ-) donation of C_n^{2-} can destabilize the 5d(Au) orbitals, but this is unlikely since Mason[27] has emphasized that all available evidence indicates ligand interactions with 5d(Au) orbitals to be weak. Moreover, the pattern of d → p transitions would be different from **3** if this mechanism is operating. For example, acetylenic π-donation would specifically destabilize $d_{xz,yz}$, but not d_{z^2} and d_{xy,x^2-y^2}. A more reasonable possibility is acetylenic π-acceptance: if $\pi*(C_n^{2-})$ is higher in energy than $p_{x,y}$(Au), this will stabilize all of the observed 5d → 6p excitations, as the low-lying ones all terminate $p_{x,y}$(Au).[24] The π* orbital of acetylene is extremely high in energy;[34] while the spin- and dipole-allowed $\pi \rightarrow \pi^*$ excitation ($^1\Sigma_g^+ \rightarrow {}^1\Sigma_u^+$) is buried under Rydberg transitions.[9]

(2) The second spectacular consequence of the bridging C_n^{2-} ligands is the observation of a near-UV electronic emission that exhibits a very sharp single vibronic progression (ν(C≡C) ≈ 2000 cm^{-1}). There is a corresponding weak absorption band with an identical origin energy but a dramatically reduced progression frequency of ~1700 cm^{-1}, plus an overlapping progression with similar vibronic structure but a higher energy origin (by ~3000 cm^{-1}). One explanation is that these features are due to [5d(Au)] → [π*(C_2)] transitions. The sharpness of the vibronic structure is inconsistent with such metal-to-ligand charge transfer (MLCT) assignment because authentic MLCT transitions typically show substantial distortions along metal−ligand coordinates. Indeed, there is an obvious assignment for these bands. It has been known for many years that electron correlation effects result in very large splitting of the six excited states that result from the one electron $\pi \rightarrow \pi^*$ excitation of a $\pi^4\pi^{*0}$ linear molecule.[34,35] A qualitative state diagram is given

(29) Because the reduction of this compound is irreversible, the reduction potential ($E_{1/2}$) is estimated from the cathodic peak potential by $E_{1/2} = E_{pc} + 0.04$ V. Note that the peak-to-peak separation of the $Cp_2Fe^{+/0}$ couple is 80 mV under this condition.

(30) Bock, C. R.; Connor, J. A.; Gutierrez, A. R.; Meyer, T. J.; Whitten, D. G.; Sullivan, B. P.; Nagle, J. K. *J. Am. Chem. Soc.* **1979**, *101*, 4815−4824.

(31) Complex **2** does not show any reductive couples even at potential of −2 V vs SSCE. It shows an irreversible oxidative wave at 1.12 V vs SSCE.

(32) Neithamer, D. R.; LaPointe, R. E.; Wheeler, R. A.; Richeson, D. S.; Van Duyne, G. D.; Wolczanski, P. T. *J. Am. Chem. Soc.* **1989**, *111*, 9056−9072.

(33) Caulton, K. G.; Cayton, R. H.; Chisholm, M. H.; Huffman, J. C.; Lobkovsky, E. B.; Xue, Z. *Organometallics* **1992**, *11*, 321−326.

(34) Buenker, R. J.; Peyerimhoff, S. D. *Chem. Rev.* **1974**, *74*, 127−188.

(35) (a) Ross, I. G. *Trans. Faraday Soc.* **1952**, *48*, 973−991. (b) Kammer, W. E. *Chem. Phys. Lett.* **1970**, *6*, 529−532. (c) Ditchfield, R.; Bene, J. D.; Pople, J. A. *J. Am. Chem. Soc.* **1972**, *94*, 4806−4811.

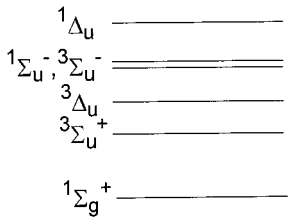

Figure 9. Qualitative $\pi \rightarrow \pi^*$ state diagram for linear C_2H_2, neglecting the very high-lying $^1\Sigma_u^+$ state.

in Figure 9. The only spin- and electronic dipole-allowed transition from the ground state occurs to the $^1\Sigma_u^+$ state, which lies at approximately double the energy of the cluster of excited states that are shown. A very high-level theoretical calculation has been reported on the lowest few *relaxed* excited states resulting from the closely spaced manifold of vertical excited states shown in Figure 9; the lowest of these was calculated at 3.49 eV (355 nm) with $^3\Sigma_u^+$ parentage, while the lowest relaxed state of $^3\Delta_u$ parentage appears at 4.18 eV (297 nm).[36]

The good energetic match with the low-energy transitions of **1** strongly suggests that they are $^3(\pi \rightarrow \pi^*)$ transitions. Hence the ~2000 cm^{-1} progression frequency in the emission spectra of **1** (Figure 3) and **2** (Figure 6) is assigned to the υ(C≡C) stretch. The ~1700 cm^{-1} progression frequency in the excitation spectra of **1** (Figure 5) is assigned to the υ(C≡C) stretch in the $^3(\pi \rightarrow \pi^*)$ excited state. There is a large change in vibrational frequency from the ground to the excited state, as is expected because of the large Franck−Condon factor (implying large distortion) indicated by the emission spectra. To the best of our knowledge, the direct experimental observation of transitions of this type for acetylenes is unprecedented in the literature, but Au(I) spin−orbit coupling effects are expected to strongly enhance their intensity even if there is no distinct π-bonding between Au(I) and the C_2^{2-} unit. Importantly, the very simple vibronic structure and the sharp υ(C≡C) progressions can be rationalized by this ligand-localized assignment. The red-shift for the analogous bands in **2** is anticipated for the conjugated C_4^{2-} bridging even though there is little experimental evidence for the corresponding hydrocarbon.[9]

Another point worth addressing is that according to calculations,[35b,36] the low-lying triplet states of C_2H_2 are strongly bent, both *cis*- and *trans*-isomers are predicted to be minima. While there is no evidence for vibronic involvement of any mode other than υ(C≡C) in the 77 K solid emission of **1**, this complex displays broad emission in room-temperature solid-state and 77 K alcoholic glasses (Figures 3 and 4, respectively). We tentatively conjecture that these emissions involve exciplex formation. One possible mechanism which is consistent with these observations is the formation of strong hydrogen bonds between the C_2 unit in the excited state and the acidic H-atoms of solvent molecules. As discussed earlier, chloroform molecules have been located around the C_2 moiety in the crystal lattice of **1**·4$CHCl_3$, and the formation of strong hydrogen bonds is likely to be a thermally activated process, since it intrinsically involves movement of $CHCl_3$ molecules within the crystal lattice. For the acetylenic $^3(\pi\pi^*)$ excited state of complex **2**, both the solid-state and solution emission spectra display a vibronic υ(C≡C) spacing. We suspect that conjugation across the C_4^{2-} chain may result in extremely low frequencies of other vibronic features other than υ(C≡C) that might not be resolved.

We have demonstrated that the strategy of employing two $Au(PCy_3)^+$ termini for the C_n^{2-} bridge has indeed afforded a long-lived and emissive acetylenic $^3(\pi\pi^*)$ excited state in solution for complex **2**. This excited state exhibits the lifetime, emission quantum yield, and excited-state reduction potential which are comparable to the prolific $^3[d\sigma^*p\sigma]$ state of $[Pt_2(P_2O_5H_2)_4]$.[4−37] Indeed, photoinduced electron-transfer reaction involving the Au−C_4−Au chain has been demonstrated. We envisage that the $^3(\pi\pi^*)$ excited state of the C_n^{2-} chains, which is "switched on" through coordination to the "heavy proton equivalent" $Au(PCy_3)^+$, will be readily manipulated to yield desirable photophysical and photochemical properties, and this will provide the impetus for future study.

Acknowledgment. We acknowledge financial support from the Research Grants Council of the Hong Kong SAR, China [HKU 7298/99P], The University of Hong Kong, and the Hong Kong University Foundation.

Supporting Information Available: Details of physical measurements, instrumentation; tables listing details of crystal data and structure refinement, atomic coordinates, calculated coordinates, isotropic and anisotropic displacement parameters, and bond length and angles for **1**·4$CHCl_3$ and **2**·2CH_2Cl_2; UV−vis absorption spectrum of **3**; a plot of $1/\tau$ vs [**2**] (PDF). This material is available free of charge via the Internet at http://pubs.acs.org.

JA001706W

(36) Wetmore, R. W.; Schaefer, H. F., III. *J. Chem. Phys.* **1978**, *69*, 1648−1654.

(37) Roundhill, D. M.; Gray, H. B.; Che, C. M. *Acc. Chem. Res.* **1989**, *22*, 55−61.